Published in final edited form as:
Hepatology. 2013 December ; 58(6): . doi:10.1002/hep.26600.

A Novel Role of Nucleostemin in Maintaining the Genome Integrity of Dividing Hepatocytes During Mouse Liver Development and Regeneration

Tao Lin[1], **Wessam Ibrahim**[1], **Cheng-Yuan Peng**[2,3], **Milton J Finegold**[4,5], and **Robert Y.L. Tsai**[1]

[1] Center for Cancer and Stem Cell Biology, Institute of Biosciences and Technology, Texas A&M Health Science Center, Houston, Texas 77030 USA

[2] School of Medicine, China Medical University, Taichung, 40402, Taiwan

[3] Division of Hepatogastroenterology, Department of Internal Medicine, China Medical University Hospital, Taichung, 40402, Taiwan

[4] Gastrointestinal & Hepatobiliary Pathology, Texas Children's Hospital Houston, Texas 77030 USA

[5] Department of Pathology & Immunology, Baylor College of Medicine, Texas 77030 USA

Abstract

During liver development and regeneration, hepatocytes undergo rapid cell division and face an increased risk of DNA damage associated with active DNA replication. The mechanism that protects proliferating hepatocytes from replication-induced DNA damage remains unclear. Nucleostemin (NS) is known to be upregulated during liver regeneration, and loss of NS is associated with increased DNA damage in cancer cells. To determine whether NS is involved in protecting the genome integrity of proliferating hepatocytes, we created an albumin promoter-driven NS conditional-null (albNS^{cko}) mouse model. Livers of albNS^{cko} mice begin to show the loss of NS in developing hepatocytes from the first postnatal week and increased DNA damage and hepatocellular injury at 1-2 weeks old. At 3-4 weeks, albNS^{cko} livers develop bile duct hyperplasia and show increased apoptotic cells, necrosis, regenerative nodules, and evidence suggestive of hepatic stem/progenitor cell (HSPC) activation. CCl_4 treatment enhances degeneration and DNA damage in NS-deleted hepatocytes and increase biliary hyperplasia and A6$^+$ cells in albNS^{cko} livers. Following 70% partial hepatectomy (PHx), albNS^{cko} livers show increased DNA damage in parallel with a blunted and prolonged regenerative response. The DNA damage in NS-depleted hepatocytes is explained by the impaired recruitment of a core DNA repair enzyme, RAD51, to replication-induced DNA damage foci. This work reveals a novel genome-protective role of NS in developing and regenerating hepatocytes.

Keywords

biliary hyperplasia; DNA damage; DNA replication; stem cells

Correspondence Contact Information: Robert Y.L. Tsai; 2121 W. Holcombe Blvd, Houston, TX 77030; (Tel): 1-713-677-7690; (Fax) 1-713-677-7512; rtsai@ibt.tamhsc.edu.
TL: tlin@ibt.tamhsc.edu WI: wessamibrahim78@yahoo.com CYP: cypeng@mail.cmuh.org.tw MJF: mjfinego@texaschildrens.org

Introduction

Fetal hepatoblasts and hepatic progenitors undergo rapid proliferation during liver organogenesis. After maturation, hepatocytes become mitotically inactive but retain the ability to reenter the cell cycle following acute liver injuries. Following massive damage, adult livers also recruit hepatic stem/progenitor cells (HSPCs) as a source for regeneration. During the process of DNA replication, spontaneous damage may occur as a result of stalled and collapsed replication forks (1, 2). To date, it remains unclear how HSPCs and proliferative hepatocytes avoid the increased risk of replication-induced DNA damage and whether molecules beyond the core DNA damage repair machinery help protect the integrity of their genome (3, 4).

Nucleostemin (NS) was discovered first in neural stem cells and later in other types of stem/progenitor cells and cancers (5, 6). The biological significance of NS is exemplified by the early embryonic lethal phenotype of germline NS-knockout (NSKO) mice (7). Its importance in stem cells is shown by NS-knockdown (NSKD)-induced self-renewal impairment and the ability of NS to promote pluripotency in conjunction with Sox2 and Oct4 (8, 9). In adult animals, the expression of NS is low in most tissues except for the testis, but is upregulated during regeneration in several tissues (10, 11). A potential role of NS in liver biology is indicated by a recent study showing an increased expression of NS in hepatic precursor cells and adult livers following partial hepatectomy (12).

As loss of NS increases spontaneous DNA damage in cancer cells (13), we hypothesize that it may have a role in protecting the genome integrity of actively dividing HSPCs and hepatocytes. To test this idea, we created a hepatocyte-specific NS conditional-knockout (albNS^{cko}) mouse model by introducing an albumin promoter-driven Cre transgene (Alb-Cre) (14) into a new NS-flox (NS^{flx}) mouse model. Because the albumin promoter gets turned on gradually during gestation and postnatal development (15), we anticipate that the albNS^{cko} model will abolish the activity of NS in the Alb^{+} differentiating hepatocytic progenitors and regenerating hepatocytes and allow us to address its role in liver development and regeneration. Indeed, livers of albNS^{cko} mice show early-onset DNA damage at 2 weeks, followed by an increase of apoptotic cells, regenerative nodules, and biliary hyperplasia at 3-4 weeks. In response to CCl_4-induced damage or PHx, albNS^{cko} livers show enhanced degeneration and DNA damage in NS-deleted hepatocytes. Mechanistically, loss of NS triggers replication-dependent DNA damage by reducing the recruitment of RAD51 to hydroxyurea (HU)-induced damage foci. These data establish a novel role of NS in protecting the genomic stability of dividing hepatocytes.

Materials and Methods

Animal Care

Animals were handled in accordance with the *Guide for the Care and Use of Laboratory Animals* and the procedures approved by the institutional Animal Care and Use Committee. For acute CCl_4 treatment, mice were injected intraperitoneally once with CCl_4 (10ul/gm BW). Oil and CCl_4-injected littermates were separately raised post injection. To perform 70% partial hepatectomy, mice were anesthetized by inhalation of isoflurane. The left lateral and medium lobe of the liver were ligated and removed.

Creation of albNS^{cko} mice

AlbNS^{cko} mice were created by crossing Alb-Cre transgenic mice (14) with NS-flox (NS^{flx}) mice. NS^{flx} mice were generated by the targeting strategy outlined in Fig. S1. Correctly targeted ES clones were identified by Southern blots. NS^{flxneo} heterozygotes were mated with Rosa26^{flp} mice (16) to remove the pgk-neo cassette and generate NS^{flx} heterozygotes.

Tissue preparation, immunohistochemistry, and TUNEL assay

Liver samples were fixed in Histochoice (Amersco) and embedded in paraffin for H&E, sirius red, anti-NS (Ab2438, 1-year-old livers), anti-CK-19 (TROMA-III, DSHB), A6 (provided by Dr. Valentina Factor at NCI), anti-γ-H2AX (JBW301, Upstate), anti-BrdU (BU1/75, Accurate), anti-α-fetoprotein (Biocare), anti-albumin (Novus), anti-Sox9 (Millipore), anti-CYP2E1 (Millipore), and TUNEL staining. For NS staining (Ab2438) in developing livers, fresh-frozen samples were collected and post-fixed in 10% formalin. The specificity of Ab2438 was validated previously (7, 17) and in Fig. S2H. Apoptotic cells were labeled by the Deadend Fluorometric TUNEL system (Promega). Nuclei were counterstained by TO-PRO®-3 (Topro-3, Invitrogen).

Hepatocyte culture, transfection, knockdown, and DNA damage analysis

See supplemental data.

Results

Alb-Cre-driven NS deletion causes liver damage associated with biliary hyperplasia

To determine the role of NS in liver regeneration, we injected 8-week-old mice with CCl_4. Northern blots showed that the expression level of NS is relatively low in the uninjured livers (Ctrl) but begins to increase shortly after the CCl_4 injection (Fig. 1A, top). NS upregulation peaks in one day and declines rapidly after two days, whereas the peak increase of BrdU-labeled cells occurs two days after the injection (Fig. 1A, bottom). We created an NS^{flx} model and showed that homozygous NS^{flx} mice develop and grow normally and homozygous deletion of the floxed sequence by a germline Cre transgene causes early embryonic lethality at E3.5 (n=110) (Fig. 1B and S1). To address the functional importance of NS in the developing hepatocytes, we generated the $albNS^{cko}$ mouse model by breeding the Alb-Cre transgene (14) into the $NS^{flx/flx}$ mice. Real-time RT-PCR assays confirm that NS expression is significantly reduced in $albNS^{cko}$ livers from 1 to 4 weeks old (Fig. 1C, top). Cre expression is found only in $albNS^{cko}$ livers and shows a prominent peak at 2 weeks old (Fig. 1C, bottom). Histologically, $albNS^{cko}$ livers appear no different from $NS^{flx/flx}$ livers up to 1 week old, but begin to show increased cellularity around bile ducts at 2 weeks of age (Fig. S2A-S2D). When $albNS^{cko}$ mice reach 3-4 weeks of age, the liver surface displays a nodular appearance (Fig. 1D) and shows areas of extensive bile duct hyperplasia (Fig. 1E1, 1E2, S2E, S2F), portal and periportal fibrosis (Fig. S2G), and necrotic foci in the parenchyma (Fig. 1E3). The liver-to-body weight ratio of $albNS^{cko}$ mice begins to exceed that of $NS^{flx/flx}$ mice at 3 weeks (Fig. 1F). These results demonstrate that NS deletion causes liver parenchymal damage and bile duct hyperplasia.

DNA damage is an early event of $albNS^{cko}$, followed by apoptosis and hepatic regeneration

To establish the onset of NS deletion and the cell type(s) involved, we examined NS expression in $albNS^{cko}$ livers from postnatal day 1 (P1D) to 3 weeks old. While a significant number of $albNS^{cko}$ hepatocytes still retain their NS expression at P1D, almost all of them lose their NS expression at 1 and 2 weeks old (Fig. 2A). These findings are consistent with a previous report that differentiated hepatocytes functionally expressing Alb-Cre are rare and distribute in a mosaic pattern in fetal livers (15). In the 2-3-week-old $albNS^{cko}$ livers, NS-positive cells are mostly confined to the hyperplastic ductular epithelium (Fig. 2B, left panels) and the regenerative hepatic nodules (Fig. 3D1). Contrarily, in the 3-week-old $NS^{flx/flx}$ liver, NS signals are found only in scattered hepatocytes but not in the bile duct epithelial cells (BECs) (Fig. 2B, right panels). Although we cannot exclude the expression of Alb-Cre in subsets of BECs, these results indicate that the expression of NS is depleted

predominantly in the hepatocytic lineage by albNS^{cko} from 1 week of age but is maintained in the hyperplastic BECs.

The time sequence of NSKO-induced events was determined by measuring the onset of DNA damage, cell death, and hepatic regeneration in albNS^{cko} livers. DNA damage in vivo was detected by the foci formation of phosphorylated histone H2AX, which plays a key role in assembling DNA damage response and repair proteins at the damage sites and provides a rapid and sensitive way to detect the DNA damage event (18). Our results showed that γ-H2AX^{+} hepatocytes are increased by albNS^{cko} as early as 1 week of age (Fig. 3A). This event peaks at 2 weeks and gradually declines afterward, coinciding with the temporal pattern of Cre expression. TUNEL assays showed that the increase of cell death occurs after the DNA damage event and peaks at 3 weeks (Fig. 3B). Compared to age-matched NS$^{flx/flx}$ mice, 2-week-old albNS^{cko} mice show a modest but significant increase in their serum levels of AST and total bilirubin (Fig. 3C). The levels of conjugated bilirubin are undetectable in both albNS^{cko} and NS$^{flx/flx}$ mice. These findings are consistent with liver parenchymal damage and not cholestasis at this early age. At 2-3 weeks old, small nodules appear in the parenchyma of albNS^{cko} livers. These nodules contain hepatocytes with more basophilic cytoplasm, NS-positive expression, more BrdU- and Ki67-labeled cells, stronger AFP signals, and less PAS staining compared to the hepatocytes outside the nodules (Fig. 3D1). At 2 weeks of age, the regenerative nodules of albNS^{cko} livers show a higher mitotic (Ki67^{+}) activity compared to NS$^{flx/flx}$ livers of the same age, whereas the peri-nodular regions show a much lower mitotic activity (Fig. S3A). These results, in conjunction with the lack of A6, Sox9, and CK-19 expression in the majority of nodular cells (Fig. S3B), indicate that these nodules contain regenerating hepatocytes but not bipotential or ductal-like progenitor cells. In contrast to the non-regenerative hepatocytes outside the nodules that contain a single large nucleolus, these newly regenerated hepatocytes contain multiple small nucleoli (Fig. 3D2). Many regenerative nodules are found in close proximity to the hyperplastic bile ductules, such as shown in the H&E and AFP panels (Fig. 3D1). To determine the spatial contiguity between the regenerative nodules and periportal areas, we performed serial sections to quantify the number of nodules that come in contact with the periportal areas versus those that do not. Of the 19 nodules traced at the age of 2-3 weeks, 16 are directly connected to the periportal region. The three that show no connection to the ductal region extend beyond the sections collected. Immunostaining showed that the junctional regions between the nodules and periportal areas contain periportal and rare single Sox9^{+} cells but not A6^{+} cells (Fig. S3C). When albNS^{cko} mice grow older than 4 weeks of age, these discrete nodules have become inconspicuous. When albNS^{cko} mice reach 12 months old, the surviving hepatocytes in their livers display pleomorphic nuclear and nucleolar morphology (Fig. 3E). At this age, NS$^{flx/flx}$ livers show scattered NS signals in a few hepatocytes but not in CK-19-labeled BECs (Fig. 3F1). In contrast, albNS^{cko} livers contain regions of mostly NS-low/negative hepatocytes (Fig. 3F2, left upper panel) and restricted areas of strong NS-positive hepatocytes intermixed with NS-low/negative cells (Fig. 3F2, bottom panel). BECs in albNS^{cko} livers still show NS-positive signals.

AlbNS^{cko} livers show signs of HPSC activation

The combination of regenerative nodules and bile duct hyperplasia suggests that HSPCs may be activated in albNS^{cko} livers. qRT-PCR assays showed that the transcript levels of several HSPC-related genes, including EpCAM, CK-19, AFP, CD-133, CD-24, and CK-7, are all significantly increased in albNS^{cko} livers compared to the age-matched NS$^{flx/flx}$ livers (Fig. 4A). The increase of HSPC-related markers is more prominent at 4 weeks old than at 1 year old. Histologically, A6-positive cells appear as early as 3-4 weeks of age in the parenchyma and the hyperplastic ductal region of albNS^{cko} livers, whereas no A6^{+}

signals are detected in $NS^{flx/flx}$ livers (Fig. 4B). The majority of the $A6^+$ cells also coexpress the CK-19 antigen on serial sections of 4um thickness (Fig. 4C).

CCl_4 increases hydropic degeneration and DNA damage in NS-depleted hepatocytes and stimulates the proliferation of $A6^+$ cells and bile ductules in $albNS^{cko}$ livers

To determine the role of NS in liver regeneration, we analyzed the responses of $albNS^{cko}$ and $NS^{flx/flx}$ livers to CCl_4 treatment at 2 weeks of age when Cre expression and DNA damage are maximal and histological changes and serum measurement of hepatocellular injury are mild in $albNS^{cko}$ livers. Liver samples were collected in pairs from CCl_4-treated and oil-treated mice at the first, second, or fourth day of the injection. $NS^{flx/flx}$ livers show acute pericentral necrosis with infiltrating leukocytes during the first two days after the injection (white arrows, Fig. 5A1). Without CCl_4 exposure, $albNS^{cko}$ livers contain regenerative nodules and non-regenerative regions (peri-nodule, Fig. 5A2). In response to CCl_4 treatment, $albNS^{cko}$ livers begin to show not only the same acute pericentral necrosis and leukocyte infiltration as seen in $NS^{flx/flx}$ livers but also severe hydropic degeneration (black arrows) in the peri-nodular areas (Fig. 5A3). Notably, the regenerative nodules are relatively resistant to the acute necrotic effect of CCl_4 treatment (Fig. 5A4), which is consistent with their lower expression of the key enzyme, cytochrome P450 (CYP2E1), that metabolizes CCl_4 and forms free radicals (Fig. S4A). Mice recover from the CCl_4-triggered pericentral necrosis after 4 days (Fig. S4B). Unlike $NS^{flx/flx}$ livers, which show no increase of $CK\text{-}19^+$ cells following CCl_4-induced damage, $albNS^{cko}$ livers display a significant increase of $CK\text{-}19^+$ bile ductules and small $CK\text{-}19^+$ progenitor-like cells located in the periportal region in response to CCl_4 treatment (Fig. 5B and S4C). Immunostaining on serial sections showed that the numbers of A6 and CK-19 double-positive progenitor cells are increased by the CCl_4 treatment in $albNS^{cko}$ livers (Fig. 5C). Consistently, the number of Sox9 and CK-19 double-positive cells is also increased in CCl_4-treated $albNS^{cko}$ livers (Fig. S4D). Supporting the idea that HSPCs may be expanded in CCl_4-treated $albNS^{cko}$ livers, qRT-PCR assays demonstrated that the mRNA levels of two HSPC-related markers, EpCAM and AFP, are both upregulated in $albNS^{cko}$ livers following CCl_4 treatment (Fig. 5D). The increase of EpCAM occurs within 1 day, peaks on the second day, and drops after 4 days, whereas the increase of AFP is found primarily on the second day of the injection. Based on the same qRT-PCR assay, we did not detect a significant increase of EpCAM or AFP in $NS^{flx/flx}$ livers during the time window of 1 to 4 days following the CCl_4 treatment, which is consistent with the idea that a single dose of CCl4 activates only a small subset of periportal progenitor cells or none (19, 20).

We then asked whether NS-depleted hepatocytes in the peri-nodular area are more susceptible to the mitotic stress caused by CCl_4-induced damage than are the NS^+ hepatocytes in the regenerative nodule. To address this question, we first measured the increase of $Ki67^+$ cells in response to CCl_4 treatment in different regions of $albNS^{cko}$ livers. In oil-treated $albNS^{cko}$ livers, most mitotic ($Ki67^+$) cells are found in the regenerative nodules (25%) and the bile duct epithelium (18%), and only a small percentage of the non-regenerative hepatocytes are $Ki\text{-}67^+$ (1.4%) (Fig. 5E). Following CCl_4 treatment, the number of mitotic cells is increased most significantly on the second day post injection in the peri-nodular hepatocytes (1.4% to 3.2%), regenerative hepatocytes (23.3% to 42.3%), and bile duct epithelium (17.4% to 25.2%) (Fig. 5E, S4E). Next, we examined whether CCl_4-induced regeneration may sensitize NS-depleted cells to DNA damage. The CCl_4 treatment itself does not elicit any DNA damage in $NS^{flx/flx}$ livers (Fig. 5F). In oil-treated $albNS^{cko}$ livers, most $\gamma\text{-}H2AX^+$ cells are found in the peri-nodular areas. Notably, CCl_4 increases the percentage of $\gamma\text{-}H2AX^+$ cells in the NS-depleted areas but not in the regenerative nodules or the bile duct epithelium (Fig. 5F).

AlbNS^{cko} livers show a significant increase of DNA damage in response to PHx

To support the CCl_4 results, we performed PHx on albNS^{cko} and NS$^{flx/flx}$ mice at 4 weeks of age. At this age, the structure of regenerative nodules in albNS^{cko} livers has become inconspicuous, and the NS-positive and negative hepatocytes are intermixed throughout most of the liver parenchyma. In response to PHx, NS$^{flx/flx}$ livers show a significant increase of Ki67^{+} cells that peaks on the second day and recovers mostly on the fourth day. Before the operation, albNS^{cko} livers contain more Ki67^{+} cells than NS$^{flx/flx}$ livers as a result of NSKO-induced liver damage and regeneration. Following PHx, albNS^{cko} livers show a blunted and prolonged regenerative response compared to NS$^{flx/flx}$ livers (Fig. 6A). While PHx increases Ki67^{+} cells but not γ -H2AX^{+} cells in NS$^{flx/flx}$ livers, it triggers a significant increase of γ-H2AX^{+} cells in albNS^{cko} livers that continues to rise 4 days after PHx in parallel with the increase of Ki67^{+} cells (Fig. 6B). The results of CCl_4 and PHx experiments both demonstrate that NS deletion predisposes regenerating hepatocytes to DNA damage.

Loss of NS triggers replication-dependent DNA damage and perturbs RAD51 recruitment to HU-induced foci in proliferating hepatocytes

Primary hepatocytes were isolated from 2-week-old NS$^{flx/flx}$ livers to determine how loss of NS predisposes developing hepatocytes to DNA damage. After two passages, cultured hepatocytes were treated with NS-specific (siNS) and control (siScr) RNAi duplexes. In the absence of external genotoxic stress, NS-knockdown (NSKD) by siNS significantly increases the percentage of γ-H2AX^{+} cells (Fig. 7A), ataxia telangiectasia and rad3 related protein (ATR)-positive cells (Fig. 7B, grey bars), and replication protein A-32 (RPA32)-positive cells (Fig. 7B, black bars). A major cause of spontaneous DNA damage is replication stalling, which triggers S-phase DNA damage. To address whether loss of NS predisposes proliferative hepatocytes to replication-dependent DNA damage, we measured the cell cycle relationship of NSKD-induced DNA damage and showed that NSKD causes a higher percentage of γ-H2AX^{+} cells in the S-phase cells than in the non-S-phase cells (Fig. 7C). This DNA damage profile resembles the effect of hydroxyurea (HU), a model agent that triggers replication stalling and DNA damage. In support, the DNA damage effect of NSKD is greatly diminished in slowly dividing hepatocytes grown under the serum deprivation condition (Fig. 7D, left panel). This lack of response to NSKD under the low serum condition is not due to a decrease of NSKD efficiency (Fig. 7D, right panel). In further support, overexpression of NS or its nucleoplasmic mutant, NSdB, both have the ability to protect proliferative hepatocytes from HU-induced DNA damage (Fig. 7E).

To establish that NS is directly engaged in the DNA damage pathway, we first demonstrated that, following the HU treatment, the endogenous NS protein in the hepatocytes forms foci in the nucleoplasm without losing its nucleolar signals, and some foci are colocalized with the γ-H2AX^{+} signal (Fig. 7F). To exclude the possibility that the DNA damage effect of NSKD may be caused secondarily by dysregulated ribosome biosynthesis, we measured the DNA damage event and the expression levels of pre-rRNAs and rRNAs in control-KD and NSKD Hep3B cells in parallel. Pre-rRNA and rRNA species were quantified by qRT-PCR on the processing site-1 (PS-1), PS-2, PS-3, and 18S rRNA sequences (Fig. S5A, left diagrams). The different PS-containing products represent precursor species that exist before the processing events occurring at different stages of pre-rRNA processing. While NSKD reduces NS transcripts and elicits a clear DNA damage response (Fig. S5B), it has no effect on the processing events occurring on PS-1, PS-2 or PS-3 (Fig. S5A, right). Neither does it reduce the amount of 18S sequence. Homologous recombination (HR) is the key repair mechanism for replication-induced DNA damage (3), and knockout of its core protein, RAD51, produces the same early embryonic lethal phenotype as does NSKO (21). We therefore reason that NS may play a role in regulating RAD51 recruitment to HU-induced DNA damage foci. To address this possibility, control-KD and NSKD hepatocytes were

treated with HU (2mM) for 24 hours and assayed for their RAD51 recruitment efficiency. In control-KD cells, HU treatment significantly increases the percentages of γ-H2AX$^+$ cells (30.7%) and RAD51$^+$ cells (38.7%) over the non-HU-treated controls (2.8% and 7.0%, respectively) (Fig. 7G). In NS-depleted hepatocytes, HU increases γ-H2AX$^+$ cells significantly (37.5%), but its effect on triggering RAD51$^+$ foci is greatly diminished (21.4%, $p<0.01$). A direct link between NSKD-induced DNA damage and perturbed RAD51 recruitment was established by the results that overexpression of RAD51 (GFP-tagged), but not that of the GFP control, is capable of partially rescuing the DNA damage phenotype of NS-depleted primary hepatocytes (Fig. 7H). These results indicate that NS depletion predisposes proliferating hepatocytes to replication-dependent DNA damage by perturbing RAD51 recruitment to DNA damage foci.

Discussion

AlbNS^{cko} triggers DNA damage and liver regeneration

The importance of NS in liver development is shown by the increase of spontaneous DNA damage, apoptosis, bile duct hyperplasia, and fibrosis in albNS^{cko} livers. DNA damage appears first in albNS^{cko} livers during the 1st-2nd postnatal week, followed by an increase of apoptotic cells that peaks at 3 weeks of age and the appearance of necrotic foci and regenerative hepatic nodules. Complete loss of NS proteins by albNS^{cko} occurs within the first week after birth and mainly affects the developing hepatocytes. Although we cannot exclude the possibility that the Alb-Cre transgene is expressed in subsets of BECs, our data indicate that most BECs do not show the Alb-Cre activity. This may explain why biliary hyperplasia becomes a prominent feature in adult albNS^{cko} livers. Newly generated hepatocytes in albNS^{cko} livers form small nodules and display basophilic cytoplasm and multiple small nucleoli. These cells also show higher mitotic activity and NS-positive expression and are less developmentally mature (as evidenced by their AFP-positive and PAS-negative staining) compared to non-regenerative hepatocytes outside the nodule. The close spatial association between the regenerative nodules and periportal areas suggests that newly generated hepatocytes may be derived from non-NS deficient BECs or HSPCs. In support, albNS^{cko} livers display increased HSPC-related proteins and the expansion of A6 and CK-19 double-positive cells. These findings suggest that HSPCs may be activated by albNS^{cko}-induced liver damage. To date, only a handful of mouse genetic models exhibit the phenotype of robust HSPC activation (22-25). Compared to those published, the albNS^{cko} model has the unique features of an early-onset expansion of HSPCs (within 4 weeks old) and long-term survival (over a year).

The role of NS in liver regeneration is shown by the increased NS expression and the response of albNS^{cko} livers to CCl_4 and PHx. In addition to the phenotypes of acute pericentral necrosis and leukocyte infiltration seen in NS$^{flx/flx}$ livers, CCl_4 triggers severe hydropic degeneration in the NS-deleted non-regenerative hepatocytes. In contrast, hepatocytes within the regenerative nodules are relatively resistant to the acute necrosis caused by CCl_4, which may be explained by their less differentiated features and lower expression of CYP2E1. Following the CCl_4-induced damage, mitotic cells are increased in the bile duct epithelium, regenerative nodules, and non-regenerative hepatocytes of albNS^{cko} livers. Although CCl_4 do not induce DNA damage in NS$^{flx/flx}$ livers, it increases DNA damage foci in albNS^{cko} livers, but only in the NS-depleted non-regenerative (peri-nodular) hepatocytes and not in the NS$^+$ regenerative nodule or bile duct epithelium. Likewise, albNS^{cko} livers show increased DNA damage in parallel with a blunted and prolonged regenerative response following PHx. These findings support a role of NS in protecting the genome integrity of regenerating hepatocytes.

Adaptation of albNS^{cko} livers to NSKO-induced damage

Despite their early-onset liver pathology, albNS^{cko} mice survive more than a year. Consistent with their Cre expression level, the DNA damage and cell death events of albNS^{cko} mice subside after 8 weeks, and their HSPC-related protein levels decrease over time as well. We propose that the transient DNA damage effect by albNS^{cko} that occurs between the first and eighth week may be the combined result of the Alb-driven Cre expression from birth to 4 weeks of age and the diminishing requirement for NS in hepatocytes as they become more mature and less mitotic. Some newly generated hepatocytes may survive the progenitor stage with a single NS allele and undergo complete knockout only after they become postmitotic. Others may adapt to the NSKO event by silencing the promoter activity of the Alb-Cre transgene or by adopting a semi-undifferentiated fate, as reported in the Alb-Cre-driven β-catenin knockout mice (26-29), thereby maintaining their NS expression in old-age livers (Fig. 3F2). Finally, how those newly generated hepatocytes differ from normal mature hepatocytes in their lifespan and metabolic function remains unclear. As aged albNS^{cko} livers display a continuous elevation of HSPC-related proteins and, hence, a sign of continuous regeneration, we speculate that the lifespan of surviving albNS^{cko} hepatocytes may be compromised.

Loss of NS predisposes proliferative hepatocytes to replication-induced DNA damage and perturbs the recruitment of RAD51

The DNA damage effect caused by NS depletion is closely linked to the DNA replication event. First, NSKD causes more DNA damage in S-phase hepatocytes than non-S-phase hepatocytes. This DNA damage profile resembles that of HU treatment. Second, NSKD has little DNA damage effect on slowly dividing hepatocytes grown under the low serum condition. Third, overexpression of NS can protect proliferative hepatocytes from DNA damage caused by HU-induced replication stalling. Our data also indicate that NS directly takes part in the DNA damage response/repair pathway based on the reasons that NSKD-induced DNA damage occurs without ribosomal perturbation and that NS protein is recruited to HU-induced nucleoplasmic foci. Importantly, we show that loss of NS does not act by increasing the source of DNA damage but by perturbing the recruitment of RAD51 to DNA damage foci that occur spontaneously, and that overexpression of RAD51 can functionally rescue the DNA damage effect of NSKD in proliferating hepatocytes. In conclusion, this study reveals an essential function of NS in maintaining the genome integrity of dividing hepatic progenitors and hepatocytes during liver organogenesis and CCl_4-induced regeneration. Loss of NS triggers replication-dependent DNA damage by a mechanism that perturbs the recruitment of RAD51 to damage-induced foci. Future studies are needed to further elucidate how NS regulates the recruitment and repair activity of RAD51.

Supplementary Material

Refer to Web version on PubMed Central for supplementary material.

Acknowledgments

We thank the Cellular & Molecular Morphology Core of the Texas Medical Center Digestive Diseases Center (NIDDK-P30-DK056338) and Pamela Parsons for help with immunohistochemistry, the Clinical Pathology Laboratory of Texas Children Hospital for liver function tests, Dr. Valentina Factor (NCI) for providing A6 antibody, and Dr. Juan Marini (BCM) for help with submandibular bleeding.

Financial Support: This work was supported in part by Texas A&M Cancer Research Council Incentive Award (RYT), NIH grant P30 DK56338 that supports the Texas Medical Center Digestive Diseases Center (RYT, MJF), and Egyptian Cultural and Educational Bureau postdoctoral fellowship (WI).

List of Abbreviations

NS	nucleostemin
albNS^{cko}	albumin promoter-driven NS conditional knockout
HSPCs	hepatic stem/progenitor cells
BECs	bile duct epithelial cells
CCl4	carbon tetrachloride
NSKO	NS-knockout
NSKD	NS-knockdown
NS^{flx}	NS-flox
Alb-Cre	albumin promoter-driven Cre
HU	hydroxyurea
BrdU	bromodeoxyuridine
P1D	postnatal day 1
TUNEL	TdT-mediated dUTP nick end labeling
AFP	α-fetoprotein
PAS	periodic acid Schiff
qRT-PCR	quantitative reverse transcription polymerase chain reaction
EpCAM	epithelial cell adhesion molecule
CK-19	cytokeratin-19
H&E	hematoxylin & eosin
ATR	ataxia telangiectasia and rad3 related protein
RPA-32	replication protein A-32
rRNA	ribosomal RNA
PS	processing site
ETS	external transcribed spacer
ITS	internal transcribed spacer
HR	homologous recombination
GFP	green fluorescent protein
PHx	70% partial hepatectomy
TO-PRO®-3	Topro-3

References

1. Saintigny Y, Delacote F, Vares G, Petitot F, Lambert S, Averbeck D, Lopez BS. Characterization of homologous recombination induced by replication inhibition in mammalian cells. Embo J. 2001; 20:3861–3870. [PubMed: 11447127]
2. Petermann E, Helleday T. Pathways of mammalian replication fork restart. Nat Rev Mol Cell Biol. 2010; 11:683–687. [PubMed: 20842177]
3. Helleday T. Amplifying tumour-specific replication lesions by DNA repair inhibitors - a new era in targeted cancer therapy. Eur J Cancer. 2008; 44:921–927. [PubMed: 18374562]

4. Ciccia A, Elledge SJ. The DNA damage response: making it safe to play with knives. Mol Cell. 2010; 40:179–204. [PubMed: 20965415]
5. Tsai RY, McKay RD. A nucleolar mechanism controlling cell proliferation in stem cells and cancer cells. Genes Dev. 2002; 16:2991–3003. [PubMed: 12464630]
6. Tsai RY, Meng L. Nucleostemin: A latecomer with new tricks. Int J Biochem Cell Biol. 2009; 41:2122–2124. [PubMed: 19501670]
7. Zhu Q, Yasumoto H, Tsai RY. Nucleostemin delays cellular senescence and negatively regulates TRF1 protein stability. Mol Cell Biol. 2006; 26:9279–9290. [PubMed: 17000763]
8. Qu J, Bishop JM. Nucleostemin maintains self-renewal of embryonic stem cells and promotes reprogramming of somatic cells to pluripotency. J Cell Biol. 2012; 197:731–745. [PubMed: 22689653]
9. Lin T, Meng L, Li Y, Tsai RY. Tumor-initiating function of nucleostemin-enriched mammary tumor cells. Cancer Res. 2010; 70:9444–9452. [PubMed: 21045149]
10. Maki N, Takechi K, Sano S, Tarui H, Sasai Y, Agata K. Rapid accumulation of nucleostemin in nucleolus during newt regeneration. Dev Dyn. 2007; 236:941–950. [PubMed: 17133523]
11. Siddiqi S, Gude N, Hosoda T, Muraski J, Rubio M, Emmanuel G, Fransioli J, et al. Myocardial induction of nucleostemin in response to postnatal growth and pathological challenge. Circ Res. 2008; 103:89–97. [PubMed: 18519946]
12. Shugo H, Ooshio T, Naito M, Naka K, Hoshii T, Tadokoro Y, Muraguchi T, et al. Nucleostemin in Injury-Induced Liver Regeneration. Stem Cells Dev. 2012; 21:3044–3054. [PubMed: 22775537]
13. Hsu JK, Lin T, Tsai RY. Nucleostemin prevents telomere damage by promoting PML-IV recruitment to SUMOylated TRF1. J Cell Biol. 2012; 197:613–624. [PubMed: 22641345]
14. Postic C, Shiota M, Niswender KD, Jetton TL, Chen Y, Moates JM, Shelton KD, et al. Dual roles for glucokinase in glucose homeostasis as determined by liver and pancreatic beta cell-specific gene knock-outs using Cre recombinase. J Biol Chem. 1999; 274:305–315. [PubMed: 9867845]
15. Weisend CM, Kundert JA, Suvorova ES, Prigge JR, Schmidt EE. Cre activity in fetal albCre mouse hepatocytes: Utility for developmental studies. Genesis. 2009; 47:789–792. [PubMed: 19830819]
16. Farley FW, Soriano P, Steffen LS, Dymecki SM. Widespread recombinase expression using FLPeR (flipper) mice. Genesis. 2000; 28:106–110. [PubMed: 11105051]
17. Meng L, Lin T, Tsai RY. Nucloplasmic mobilization of nucleostemin stabilizes MDM2 and promotes G2-M progression and cell survival. J Cell Sci. 2008; 121:4037–4046. [PubMed: 19033382]
18. Podhorecka M, Skladanowski A, Bozko P. H2AX Phosphorylation: Its Role in DNA Damage Response and Cancer Therapy. J Nucleic Acids. 2011; 2011:1–9.
19. Huch M, Dorrell C, Boj SF, van Es JH, Li VS, van de Wetering M, Sato T, et al. In vitro expansion of single Lgr5+ liver stem cells induced by Wnt-driven regeneration. Nature. 2013; 494:247–250. [PubMed: 23354049]
20. Malato Y, Naqvi S, Schurmann N, Ng R, Wang B, Zape J, Kay MA, et al. Fate tracing of mature hepatocytes in mouse liver homeostasis and regeneration. J Clin Invest. 2011; 121:4850–4860. [PubMed: 22105172]
21. Tsuzuki T, Fujii Y, Sakumi K, Tominaga Y, Nakao K, Sekiguchi M, Matsushiro A, et al. Targeted disruption of the Rad51 gene leads to lethality in embryonic mice. Proc Natl Acad Sci U S A. 1996; 93:6236–6240. [PubMed: 8692798]
22. Lu L, Li Y, Kim SM, Bossuyt W, Liu P, Qiu Q, Wang Y, et al. Hippo signaling is a potent in vivo growth and tumor suppressor pathway in the mammalian liver. Proc Natl Acad Sci U S A. 2010; 107:1437–1442. [PubMed: 20080689]
23. Endo Y, Zhang M, Yamaji S, Cang Y. Genetic abolishment of hepatocyte proliferation activates hepatic stem cells. PLoS One. 2012; 7:e31846. [PubMed: 22384083]
24. Jakubowski A, Ambrose C, Parr M, Lincecum JM, Wang MZ, Zheng TS, Browning B, et al. TWEAK induces liver progenitor cell proliferation. J Clin Invest. 2005; 115:2330–2340. [PubMed: 16110324]

25. Benhamouche S, Curto M, Saotome I, Gladden AB, Liu CH, Giovannini M, McClatchey AI. Nf2/Merlin controls progenitor homeostasis and tumorigenesis in the liver. Genes Dev. 2010; 24:1718–1730. [PubMed: 20675406]

26. Braeuning A, Singh Y, Rignall B, Buchmann A, Hammad S, Othman A, von Recklinghausen I, et al. Phenotype and growth behavior of residual beta-catenin-positive hepatocytes in livers of beta-catenin-deficient mice. Histochem Cell Biol. 2010; 134:469–481. [PubMed: 20886225]

27. Sekine S, Ogawa R, Kanai Y. Hepatomas with activating Ctnnb1 mutations in 'Ctnnb1-deficient' livers: a tricky aspect of a conditional knockout mouse model. Carcinogenesis. 2011; 32:622–628. [PubMed: 21216847]

28. Thompson MD, Wickline ED, Bowen WB, Lu A, Singh S, Misse A, Monga SP. Spontaneous repopulation of beta-catenin null livers with beta-catenin-positive hepatocytes after chronic murine liver injury. Hepatology. 2011; 54:1333–1343. [PubMed: 21721031]

29. Wang EY, Yeh SH, Tsai TF, Huang HP, Jeng YM, Lin WH, Chen WC, et al. Depletion of beta-catenin from mature hepatocytes of mice promotes expansion of hepatic progenitor cells and tumor development. Proc Natl Acad Sci U S A. 2011; 108:18384–18389. [PubMed: 22042854]

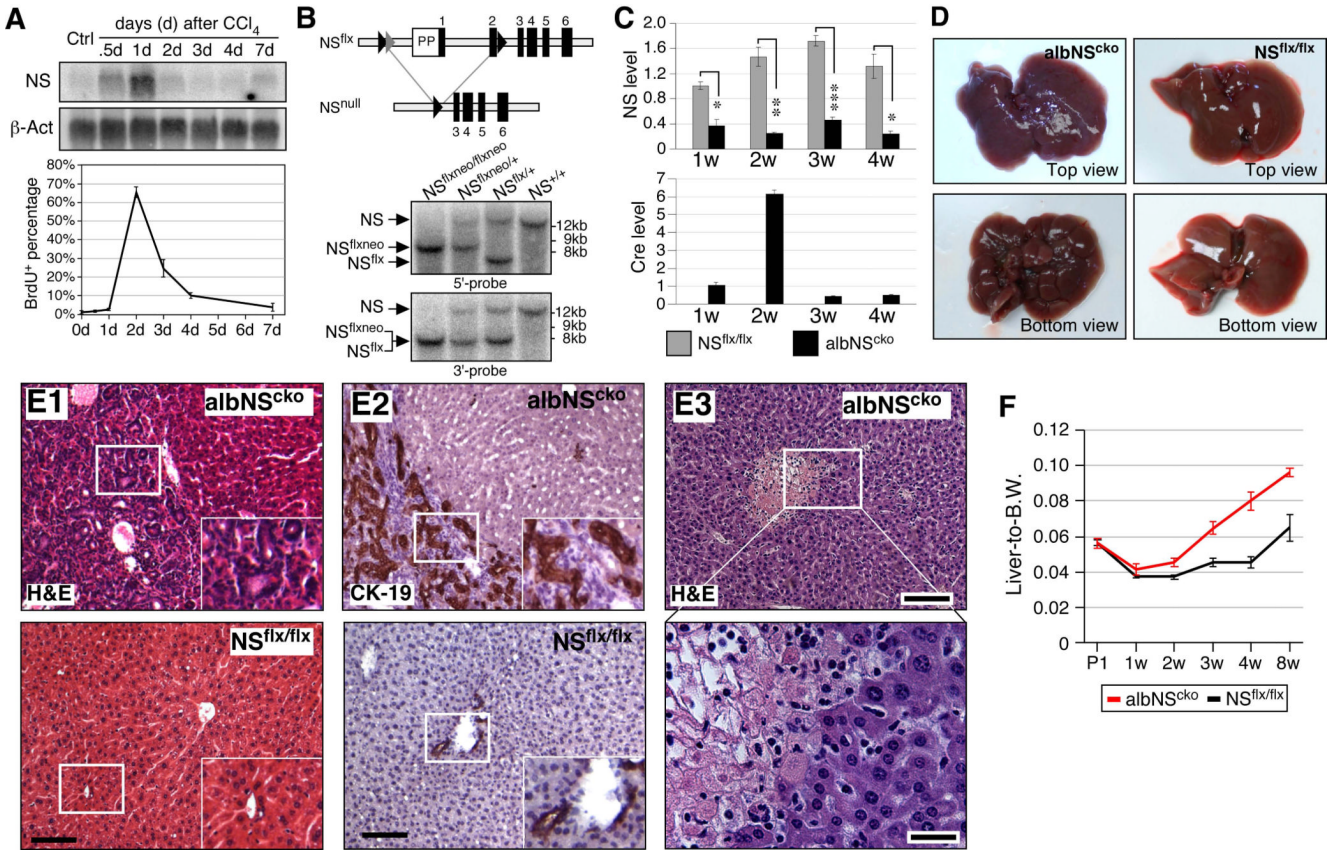

Figure 1. Alb-Cre-driven NS deletion causes liver damage associated with bile duct hyperplasia

(**A**) (Top) Northern blots show a significant upregulation of NS transcripts in CCl_4-injured livers (8-week-old). The increase of NS peaks on the first day of the injection. (Bottom) the percentage of BrdU-labeled hepatocytes reaches plateau on the second day of the injection. (**B**) Southern blots (hybridized with 5'-probe or 3'-probe) confirm the genotypes of the NS^{flxneo} and NS^{flx} alleles. (**C**) qRT-PCR assays verify the decrease of NS (top) and the increase of Cre (bottom) in $albNS^{cko}$ livers compared to age-matched $NS^{flx/flx}$ livers from 1 to 4 weeks old. (**D**) At 4 weeks, $albNS^{cko}$ livers display a nodular appearance. (**E1**) The H&E histology of 4-week-old $albNS^{cko}$ livers shows hepatic lobules surrounded by hyperplastic bile ducts. Insets show enlarged images of the rectangles. (**E2**) These hyperplastic bile ducts express CK-19. Bottom panels show images of $NS^{flx/flx}$ livers. (**E3**) From 3 weeks of age, necrotic foci can be seen in the $albNS^{cko}$ liver parenchyma. The bottom panel shows an enlarged view of the rectangular region in the top panel. (**F**) The liver-to-body weight ratio of $albNS^{cko}$ mice increases over that of $NS^{flx/flx}$ mice from 3 weeks old. Bar and line graphs represent mean ± SEM. *, $p < 0.01$, **, $p < 0.001$, ***, $p < 0.0001$. Scale bars, 100um in (**E1, E2, E3** top) and 25um in (**E3** bottom).

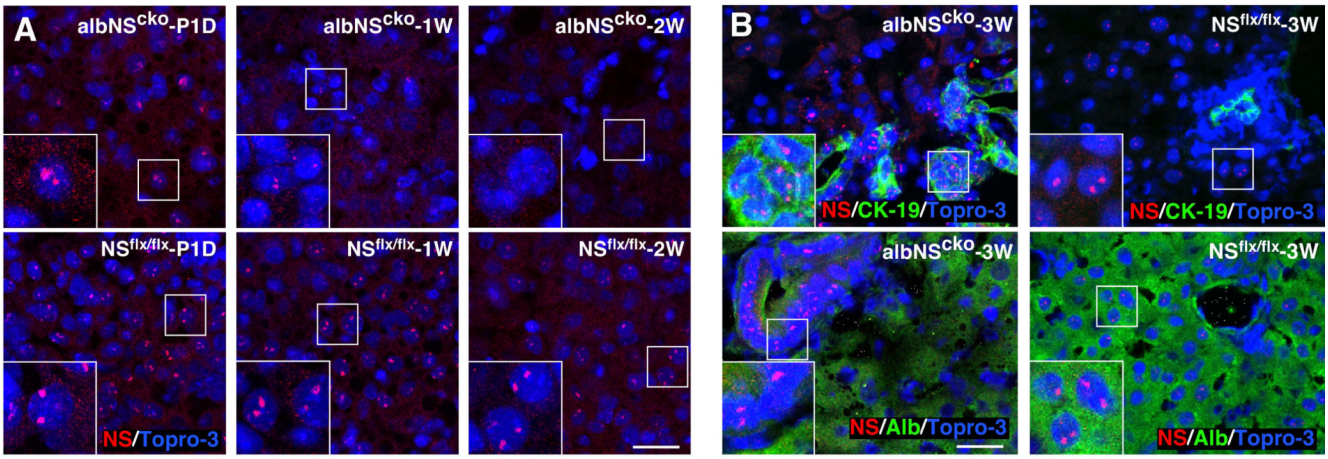

Figure 2. Loss of NS protein in albNS^{cko} livers by immunofluorescence

(**A**) A significant number of albNS^{cko} hepatocytes still retains NS expression at postnatal day 1 (P1D). Starting from 1 and 2 weeks old (1W and 2W), most albNS^{cko} hepatocytes completely lose their NS expression. (**B**) In 3-week-old albNS^{cko} livers (albNS^{cko}-3W), strong NS signals are found in the hyperplastic ductular epithelium (CK-19^{+}) and absent in the Alb^{+} hepatocytes. In 3-week-old NS$^{flx/flx}$ livers (NS$^{flx/flx}$-3W), NS signals are found in scattered hepatocytes but not in the bile duct epithelium. Insets show enlarged images of the square regions. Scale bars, 25um.

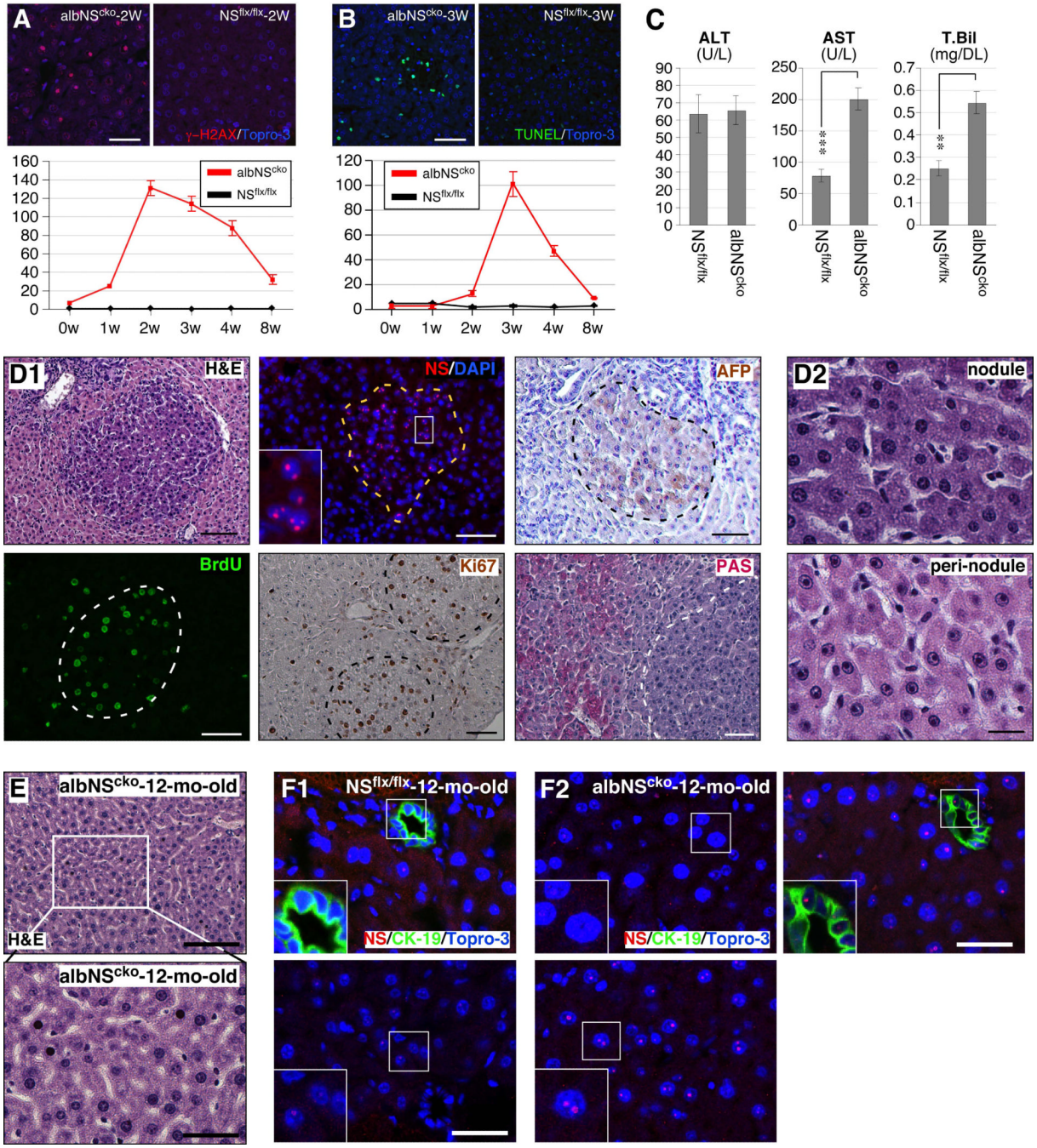

Figure 3. DNA damage is an early event of albNS^{cko}, followed by apoptosis and hepatic regeneration

(**A**) Alb-Cre-driven NSKO (albNS^{cko}) leads to a sharp increase of γ-H2AX^{+} hepatocytes that peaks at 2 weeks and declines between 3 and 8 weeks of age. Y-axis shows the number of cells per 0.01mm^2 (mean ± SEM). (**B**) AlbNS^{cko} increases the number of apoptotic hepatocytes (green, TUNEL staining) at a later time point (3-4 weeks old). Y-axis represents cell number per 0.01mm^2. (**C**) At 2 weeks old, albNS^{cko} mice show a significant increase in their serum levels of AST and total bilirubin (T. Bil) compared to age-matched NS$^{flx/flx}$ mice. The ALT levels are the same and the direct (conjugated) bilirubin levels are undetectable in both groups. ** and *** represent p values < 0.001 and 0.0001, respectively.

(**D1**) At 2-3 weeks of age, small basophilic nodules begin to appear in the albNS^{cko} liver parenchyma (H&E). Most hepatocytes inside these nodules (demarcated by dash lines) express NS, remain mitotically active (BrdU-labeled and Ki67^{+}), and are not fully differentiated, as indicated by their α-fetoprotein^{+} (AFP^{+}) expression. The PAS^{-} staining pattern reveals loss of glycogen from the nodules. Inset shows an enlarged image of the NS signal. (**D2**) These newly generated hepatocytes within the nodules show basophilic cytoplasm and nuclear hyperchromasia. In contrast, the hepatocytes outside the nodules (peri-nodule) exhibit acidophilic cytoplasm, normal chromatin, and a single large nucleolus. (**E**) Surviving hepatocytes in 1-year-old albNS^{cko} livers display mild nuclear pleomorphism. (**F**) At 1 year, NS$^{flx/flx}$ livers show scattered NS signals in a few hepatocytes but not in CK-19^{+} bile duct epithelial cells (BECs) (**F1**), whereas albNS^{cko} livers contain regions of mostly NS-negative or low hepatocytes (**F2**, left upper panel) and restricted areas of strong NS-positive hepatocytes intermixed with NS-negative or low cells (**F2**, bottom panel). At this age, BECs of albNS^{cko} livers still show NS-positive signals (**F3**, right upper panel). Bars, 50um in (**A, B, D1**), 20um in (**D2**), 100um in (**E** top panel), and 40um in (**E** bottom panel, **F**).

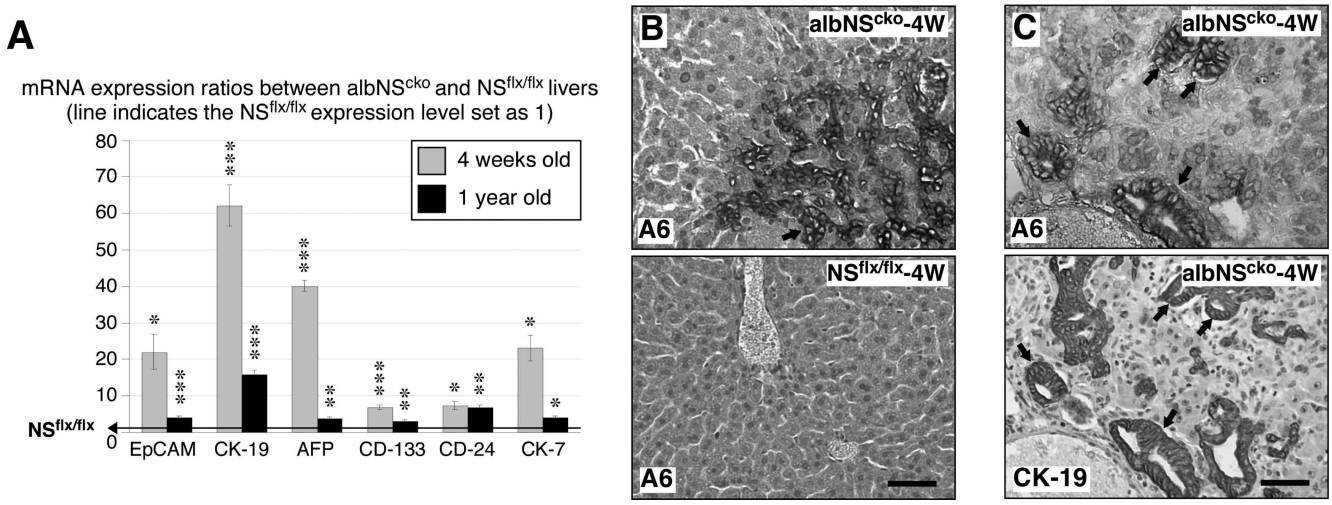

Figure 4. AlbNS^{cko} livers show signs of hepatic stem/progenitor cell (HSPC) activation

(**A**) Real-time RT-PCR assays show that the transcript levels of several HSPC-related genes are increased in albNS^{cko} livers compared to their age-matched NS$^{flx/flx}$ controls at 4 weeks (grey) and 1 year old (black). Bar graphs show the albNS^{cko}-to-NS$^{flx/flx}$ ratios of HSPC-related protein expression. Asterisks represent the p values (see Fig. 1). (**B**) At 4 weeks old, A6^{+} progenitor cells (arrow) appear in the parenchyma and hyperplastic ductular areas of albNS^{cko} livers. No A6^{+} signal can be found in NS$^{flx/flx}$ livers. (**C**) The majority of the A6^{+} progenitors also coexpress the CK-19 antigen on serial sections (arrows). Scale bars, 50um.

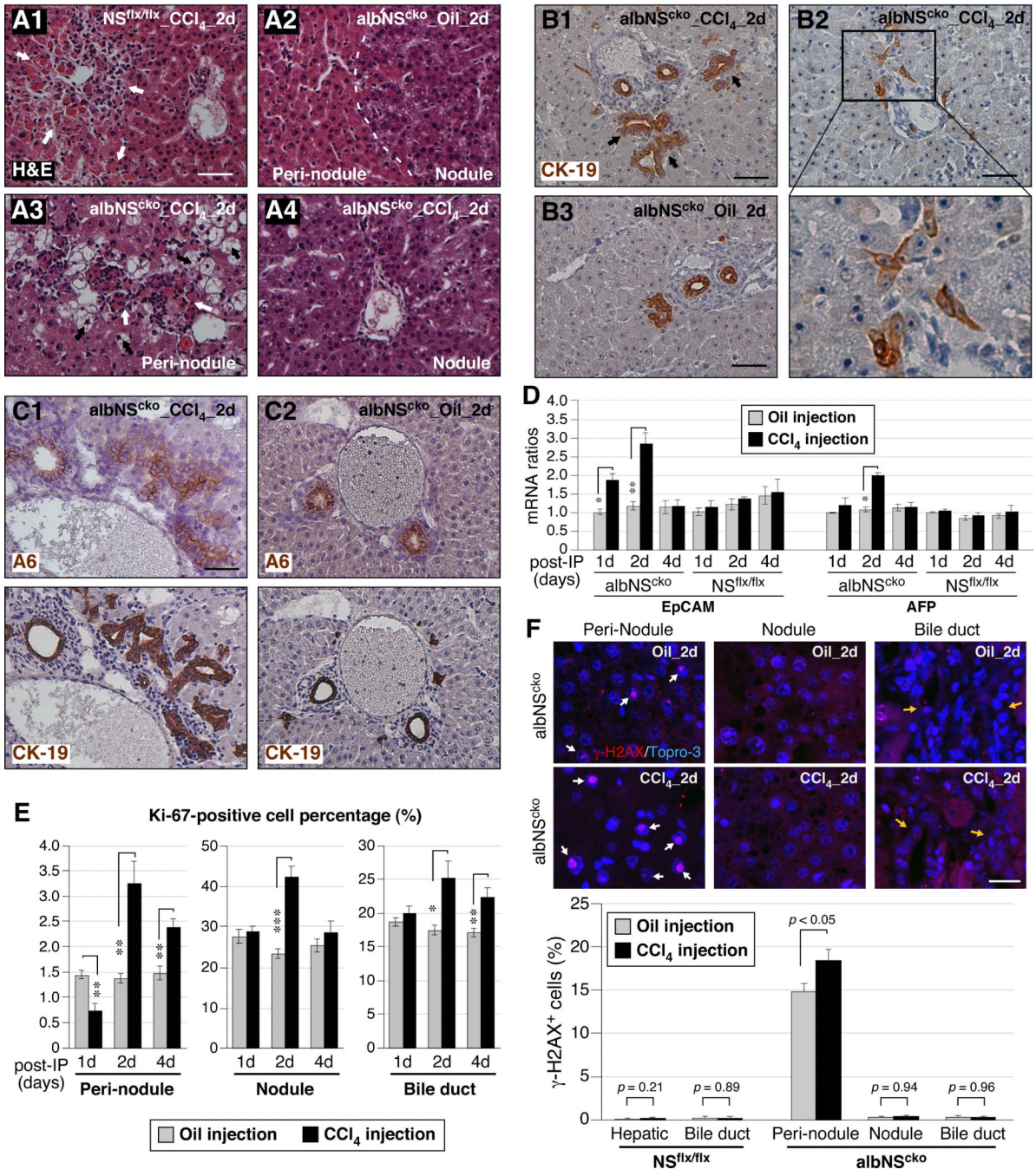

Figure 5. CCl_4 increases hydropic degeneration and DNA damage in NS-depleted hepatocytes and enhances $A6^+$ cell expansion and biliary hyperplasia in $albNS^{cko}$ livers

(**A**) Mice are injected with CCl_4 at 2 weeks of age and analyzed on the first, second, and fourth day post injection. H&E staining shows that CCl_4 causes acute pericentral necrosis and leukocyte infiltration (indicated by white arrows) in both $NS^{flx/flx}$ (**A1**) and $albNS^{cko}$ livers (**A3**) during the first 2 days of the injection. CCl_4 triggers hydropic degeneration (indicated by black arrows) of hepatocytes specifically in the peri-nodular regions of $albNS^{cko}$ livers. Bars, 100um. (**B**) In response to CCl_4 treatment, $albNS^{cko}$ livers also display a notable increase of $CK\text{-}19^+$ ducts (**B1**, arrows) and scattered progenitor-like cells (**B2**), both of which are not seen in CCl_4-treated $NS^{flx/flx}$ livers (**B3**). (**C**) Immunostaining

on serial sections of 4um thickness shows that A6 and CK-19 double-positive progenitor cells are increased significantly in CCl_4-treated albNS^{cko} livers (**C1**) compared to oil-treated albNS^{cko} livers (**C2**). (**D**) qRT-PCR assays showed that CCl_4-induced damage upregulates the transcript levels of both EpCAM and AFP in albNS^{cko} livers but not in NS$^{flx/flx}$ livers. Asterisks represent p values (described in Fig. 1). (**E**) In oil-treated albNS^{cko} livers (grey bars), most Ki67^{+} cells are found in the regenerative nodules and the bile duct epithelium, and only a small percentage of the non-regenerative hepatocytes in peri-nodular regions are Ki-67^{+}. Following CCl_4 treatment, mitotic cells are increased most significantly on the second day post injection in the peri-nodular areas, regenerative nodules, and bile duct epithelium. (**F**) Most γ-H2AX^{+} cells (indicated by white arrows) in oil-treated albNS^{cko} livers are found in the peri-nodular areas. On the second day post injection, CCl_4 increases γ-H2AX^{+} cells only in the peri-nodular regions of albNS^{cko} livers where NS is deleted but not in the regenerative nodules or the bile duct epithelium (indicated by yellow arrows). The CCl_4 treatment itself does not cause any DNA damage in NS$^{flx/flx}$ livers. Scale bars, 50um in (**A, B**, and **C**) and 20um in (**F**).

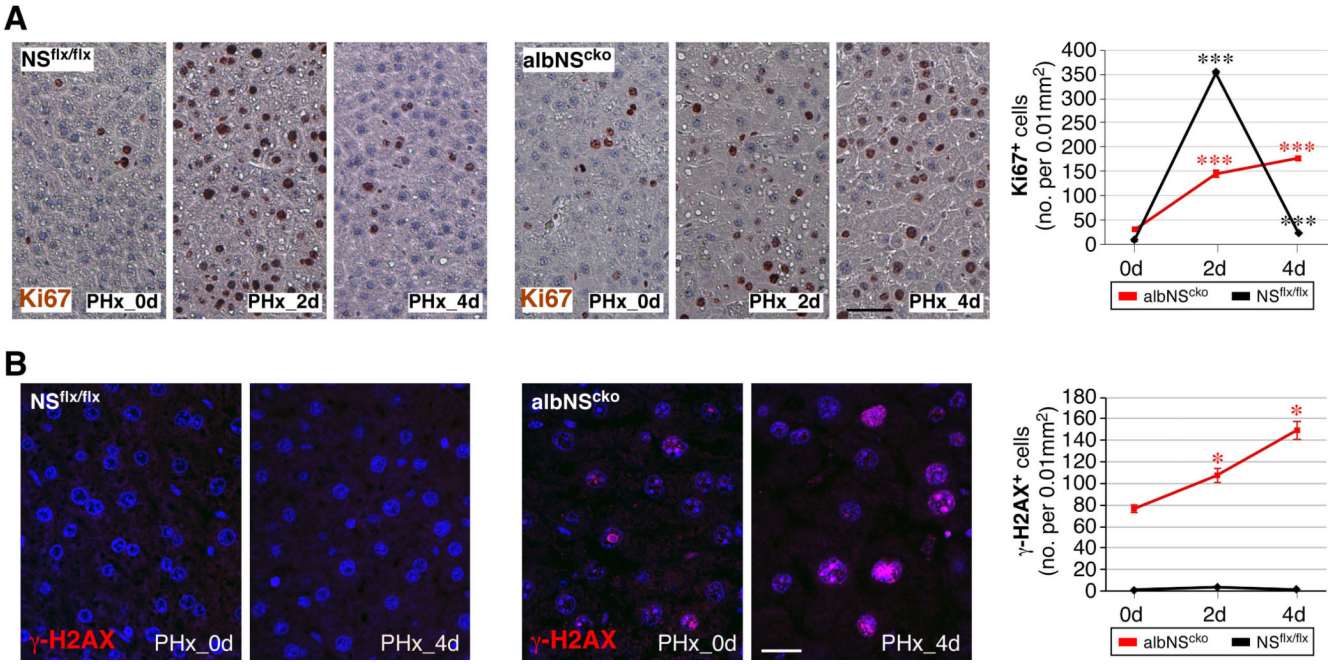

Figure 6. 70% partial hepatectomy (PHx) increases DNA damage in hepatocytes in 4-week-old albNS^{cko} livers

Mice received PHx at 4 weeks of age, and their liver samples were analyzed before the operation (PHx_0d), on the second day (PHx_2d) and fourth day (PHx_4d) after the operation. (**A**) In response to PHx, NS$^{flx/flx}$ livers show a significant increase of Ki67^{+} cells that peaks on the second day and recovers mostly on the fourth day. Before the operation, albNS^{cko} livers contain more Ki67^{+} cells than NS$^{flx/flx}$ livers. Following PHx, albNS^{cko} livers show a blunted and prolonged regenerative response compared to NS$^{flx/flx}$ livers. (**B**) Two days after PHx, albNS^{cko} livers show a significant increase of γ-H2AX^{+} cells and the number of γ-H2AX^{+} cells continues to increase 4 days after PHx (PHx_4d). In contrast, PHx does not increases γ-H2AX^{+} cells in NS$^{flx/flx}$ livers. Y-axis shows the number of γ-H2AX^{+} cells per 0.01mm^2 (mean ± SEM). * and *** indicate $p < 0.05$ and 0.0001, respectively. Scale bars, 50um in (**A**) and 20um in (**B**).

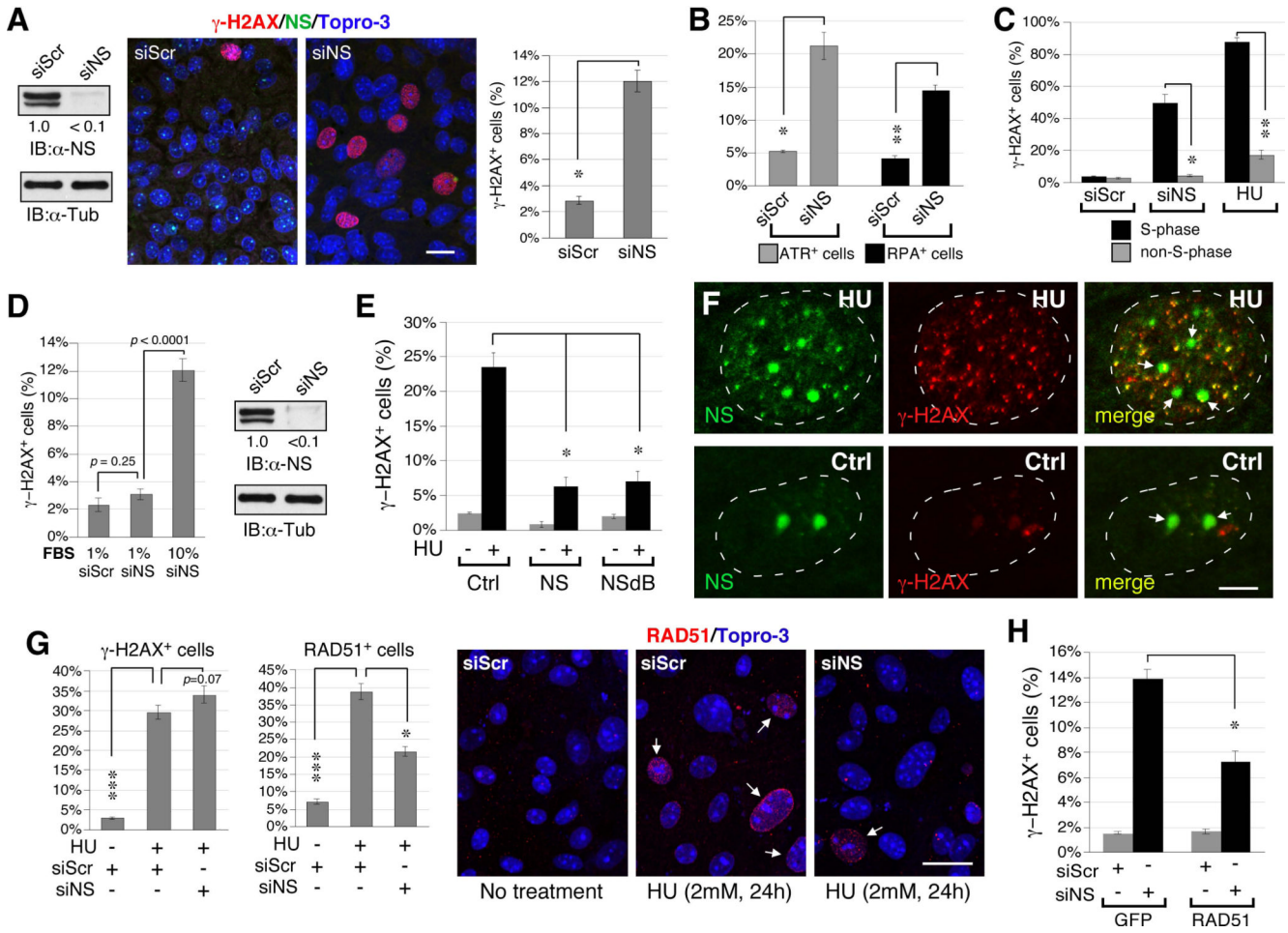

Figure 7. NS depletion triggers replication-dependent DNA damage and impairs RAD51 recruitment to HU-induced foci in proliferating hepatocytes

(**A**) Compared to control knockdown by siScr, NS-knockdown (NSKD) by siNS increases the percentage of γ-H2AX$^+$ cells (red) in primary hepatocytes isolated from 2-week-old NS$^{flx/flx}$ livers. Samples were co-labeled with anti-NS (green) and Topro-3 staining (blue). The knockdown efficiency of NS protein is >90%. Scale bar, 20um. (**B**) NSKD also increases the percentages of ATR$^+$ (grey bars) and RPA32$^+$ hepatocytes (black bars). (**C**) NSKD has a much stronger effect in triggering DNA damage (γ-H2AX$^+$ foci) in S-phase cells (BrdU$^+$) than in non-S-phase cells. This DNA damage profile resembles the effect of HU. (**D**) NSKD elicits little or no DNA damage in hepatocytes grown under the low serum (1%) condition, which lowers the proliferative rate of hepatocytes without reducing the NSKD efficiency. (**E**) Overexpression of wildtype NS or NSdB (a nucleoplasmic NS mutant) can both protect primary hepatocytes from HU-induced γ-H2AX$^+$ damage foci. (**F**) HU treatment of primary hepatocytes induces foci formation of endogenous NS (Ab2438, green) in the nucleoplasm, some of which colocalizes with the γ-H2AX signal (red). Arrows indicate the nucleoli. Scale bars, 5um. (**G**) In siScr-KD hepatocytes, HU treatment significantly increases the percentages of γ-H2AX$^+$ and RAD51$^+$ foci. In NS-depleted hepatocytes, HU increases the percentage of γ-H2AX$^+$ cells, but its effect on triggering RAD51 foci formation is greatly attenuated. Arrows indicate cells with RAD51$^+$ foci. (**H**) Overexpression of RAD51 can partially rescue the DNA damage (γ-H2AX$^+$) phenotype of NS-depleted hepatocytes. Bar graphs, mean ± SEM.